

¹⁵N CIDNP Study of Formation and Decay of Peroxynitric Acid: Evidence for Formation of Hydroxyl Radicals

Manfred Lehnig,^{*†} Michael Kirsch,^{*‡} and Hans-Gert Korth[§]

Organische Chemie, Fachbereich Chemie, Universität Dortmund, D-44221 Dortmund, Germany, Institut für Physiologische Chemie, Universitätsklinikum Essen, Hufelandstrasse 55, D-45122 Essen, Germany, and Institut für Organische Chemie, Universität Duisburg-Essen, Universitätsstrasse 5, D-45117 Essen, Germany

Received November 4, 2002

The reaction of nitrous acid with hydrogen peroxide leads to nitric acid as the only stable product. In the course of this reaction, peroxynitrous acid (ONOOH) and, in the presence of CO₂, a peroxynitrite–CO₂ adduct (ONOOCO₂[−]) are intermediately formed. Both intermediates decompose to yield highly oxidizing radicals, which subsequently react with excess hydrogen peroxide to yield peroxynitric acid (O₂NOOH) as a further intermediate. During these reactions, ¹⁵N chemically induced dynamic nuclear polarization (CIDNP) effects are observed, the analysis of the pH dependency of which allows the elucidation of mechanistic details. The formation and decay of peroxynitric acid via free radicals NO₂[•] and HOO[•] is demonstrated by the appearance of ¹⁵N CIDNP leading to emission (E) in the ¹⁵N NMR signal of O₂NOOH during its formation and to enhanced absorption (A) during its decay reaction. Additionally, the ¹⁵N NMR signal of the nitrate ion (NO₃[−]) appears in emission at pH ~ 4.5. These observations are explained by proposing the intermediate formation of short-lived radical anions O₂NOOH^{•−} probably generated by electron transfer between peroxynitric acid and peroxynitrate anion, followed by decomposition of O₂NOOH^{•−} into NO₃[−] and HO[•] and NO₂[−] and HOO[•] radicals, respectively. The feasibility of such reactions is supported by quantum-chemical calculations at the CBS-Q level of theory including PCM solvation model corrections for aqueous solution. The release of free HO[•] radicals during decomposition of O₂NOOH is supported by ¹³C and ¹H NMR product studies of the reaction of preformed peroxynitric acid with [¹³C₂]DMSO (to yield the typical “HO[•] products” methanesulfonic acid, methanol, and nitromethane) and by ESR spectroscopic detection of the HO[•] and CH₃[•] radical adducts to the spin trap compound POBN in the absence and presence of isotopically labeled DMSO, respectively.

Introduction

Peroxynitric acid (O₂NOOH/O₂NOO[−]; pK_a = 5.8) finds growing interest because of its presence in the Earth's atmosphere where it is formed by combination of free hydroperoxyl radicals, HOO[•], and nitrogen dioxide, NO₂[•].^{1,2}



Besides its formation via reaction 1, peroxynitric acid has also been found to be produced as an unstable intermediate from reaction of N₂O₅ with excess H₂O₂ (eq 2)^{3–5} and of nitrous acid with H₂O₂ (eq 3).⁶



Peroxynitric acid might also be of physiological importance as a recombination product of endogenously produced superoxide (HOO[•]/O₂^{•−}; pK_a = 4.8) and NO₂[•].⁷ Its formation

* To whom correspondence should be addressed. E-mail: lehnig@chemie.uni-dortmund.de (M.L.); michael.kirsch@uni-essen.de (M.K.). Fax: (+49)231-755-5363 (M.L.).

[†] Universität Dortmund.

[‡] Universitätsklinikum Essen.

[§] Universität Duisburg-Essen.

(1) Cantrell, C. A. In *N-centered Radicals*; Agassi, Z. B., Ed.; J. Wiley: Chichester, U.K., 1998; p 371.

(2) Wallington, T. J.; Nielsen, O. J. In *Peroxyl Radicals*; Agassi, Z. B., Ed.; J. Wiley: Chichester, U.K., 1997; p 457.

(3) Kenley, R. A.; Trevor, P. L.; Lan, B. Y. *J. Am. Chem. Soc.* **1981**, *103*, 2203–2206.

(4) D'Ans, J.; Friederich, W. *Z. Anorg. Chem.* **1911**, *73*, 325–359.

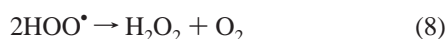
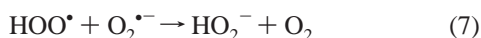
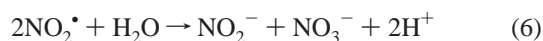
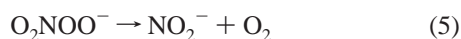
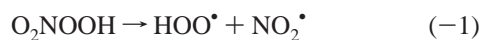
(5) Schwarz, R. *Z. Anorg. Chem.* **1948**, *256*, 3–9.

(6) Appelman, H.; Gosztola, D. *J. Inorg. Chem.* **1995**, *34*, 787–791.

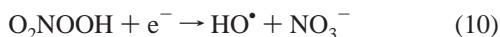
according to reactions 1 and/or 4 and subsequent decomposition has been suggested to be an effective detoxification mechanism for NO_2^\bullet in living organisms.^{8,9}



The decay reactions of peroxyntic acid are rather complex and are not understood in all details. In solution, the thermal decay of peroxyntic acid and its anion occurs via unimolecular decomposition (eqs -1, -4, and 5) giving nitrous acid, nitric acid, oxygen, and hydrogen peroxide (eqs 6–8).^{3,10–13}



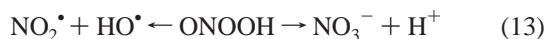
Additionally, peroxyntic acid might oxidize nitrite to nitrate (eq 9),¹² and one-electron reduction of O_2NOOH has been proposed to be a source of hydroxyl radicals (eq 10).¹³



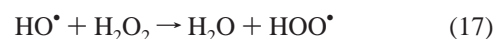
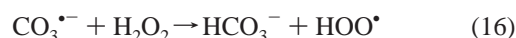
Reaction of nitrous acid with hydrogen peroxide yields peroxyntic acid ($\text{ONOOH}/\text{ONO}^-$; $\text{p}K_a = 6.5$) as an unstable intermediate ($k_{\text{dec}}^{298\text{K}} = 1.3 \text{ s}^{-1}$).^{6,14–16}



It is now well established that peroxyntic acid is a precursor of peroxyntic acid in the course of the reaction of nitrous acid with hydrogen peroxide (eqs 11 and 12). Peroxyntic acid decomposes homolytically to free hydroxyl radicals and nitrogen dioxide and isomerizes to nitrate (eq 13).^{14,17}



The release of free radicals HO^\bullet and NO_2^\bullet during the decay of peroxyntic acid, however, is still a matter of debate.¹⁸ In any case, consensus exists that the decomposition of peroxyntic acid is mediated by traces of CO_2 via a putative intermediate, ONOOCO_2^- , which is reasonably formed by nucleophilic addition of peroxyntic acid to CO_2 .^{19,20} The peroxyntic acid– CO_2 adduct decomposes rapidly ($t_{1/2} \leq 10^{-5} \text{ s}^{-1}$)⁸ to NO_2^\bullet and $\text{CO}_3^{\bullet-}$ radicals, which further might react via (formal) O^\bullet transfer to NO_3^- (eqs 14 and 15).^{19,20} In the presence of hydrogen peroxide, HOO^\bullet radicals are formed via reactions 16 and 17.^{21,22}



Peroxyntic acid has been proposed to cause tissue injuries during inflammatory and infectious diseases.²³ 3-Nitrotyrosine has been detected during pathological events and discussed as a marker for reactions of peroxyntic acid with biological systems.²⁴ Therefore, the reactions of peroxyntic acid with biological targets, especially with tyrosine, are of great interest. In previous reports, ¹⁵N CIDNP (chemically induced dynamic nuclear polarization) investigations during decomposition of peroxyntic acid and the peroxyntic acid– CO_2 adduct and during nitration of tyrosine at various pH values have been performed by us and others.^{8,25–29} At pH 5.25 and 4.5, peroxyntic acid has been generated in situ by reaction of ¹⁵N-enriched sodium nitrite with hydrogen peroxide (eq 11).²⁶

The appearance of CIDNP effects, that is, the occurrence of emission (E) and/or enhanced absorption signals (A) in the NMR spectra of the products formed from fast radical reactions unequivocally proves product formation via radical pairs and serves as a very valuable tool for the elucidation

- (14) Halfpenny, E.; Robinson, P. L. *J. Chem. Soc.* **1952**, 928–938.
 (15) Hughes, M. N.; Nicklin, H. G. *J. Chem. Soc. A* **1968**, 450–452.
 (16) Logager, T.; Sehested, K. *J. Phys. Chem.* **1993**, *97*, 10047–10052.
 (17) Hodges, G. R.; Ingold, K. U. *J. Am. Chem. Soc.* **1999**, *121*, 10695–10701.
 (18) Kissner, R.; Koppenol, W. H. *J. Am. Chem. Soc.* **2002**, *124*, 234–239.
 (19) Lyman, S. V.; Hurst, J. K. *J. Am. Chem. Soc.* **1995**, *117*, 8867–8868.
 (20) Coddington, J. W.; Wherland, S.; Hurst, J. K. *Inorg. Chem.* **2001**, *40*, 528–532.
 (21) Thomas, J. K. *Adv. Radiat. Chem.* **1969**, *1*, 103–198.
 (22) Behar, D.; Czapski, G. J.; Duchovny, I. *J. Phys. Chem.* **1970**, *74*, 2206–2210.
 (23) Beckman, J.; Beckman, T. W.; Chen, J.; Marshall, P. A.; Freeman, B. A. *Proc. Natl. Acad. Sci. U.S.A.* **1990**, *87*, 1620–1624.
 (24) Ischiropoulos, H.; Zhu, L.; Chen, J.; Tsai, M.; Martin, J. C.; Smith, C. D.; Beckman, J. S. *Arch. Biochem. Biophys.* **1992**, *298*, 431–437.
 (25) Butler, A. R.; Rutherford, T. J.; Short, D. M.; Ridd, J. H. *Chem. Commun.* **1997**, 669–670.
 (26) Lehning, M. *Arch. Biochem. Biophys.* **1999**, *368*, 303–318.
 (27) Lehning, M.; Jakobi, K. *J. Chem. Soc., Perkin Trans. 2* **2000**, 2016–2021.
 (28) Butler, A. R.; Rutherford, T. J.; Short, D. M.; Ridd, J. H. *Nitric Oxide: Biol. Chem.* **2000**, *4*, 472–482.
 (29) Lehning, M. *Arch. Biochem. Biophys.* **2001**, *393*, 245–254.

(7) Halliwell, B.; Gutteridge, M. C. *Free Radicals in Biology and Medicine*, 3rd ed.; University Press: Oxford, U.K., 1999; p 99.

(8) Kirsch, M.; Lehning, M.; Korth, H.-G.; Sustmann, R.; de Groot, H. *Chem.—Eur. J.* **2001**, *7*, 3313–3320.

(9) Kirsch, M.; de Groot, H. *J. Biol. Chem.* **2000**, *275*, 16702–16708.

(10) Sutton, H. C.; Seddon, W. A.; Sopchysyn, F. C. *Can. J. Chem.* **1978**, *56*, 1961–1964.

(11) Lammel, G.; Perner, D.; Warneck, P. *J. Phys. Chem.* **1990**, *94*(4), 6141–6144.

(12) Regimbal, J.-M.; Mozurkewich, M. *J. Phys. Chem. A* **1997**, *101*, 8822–8829.

(13) Goldstein, S.; Czapski, G.; Lind, J.; Merenyi, G. *Inorg. Chem.* **1998**, *37*, 3943–3947.

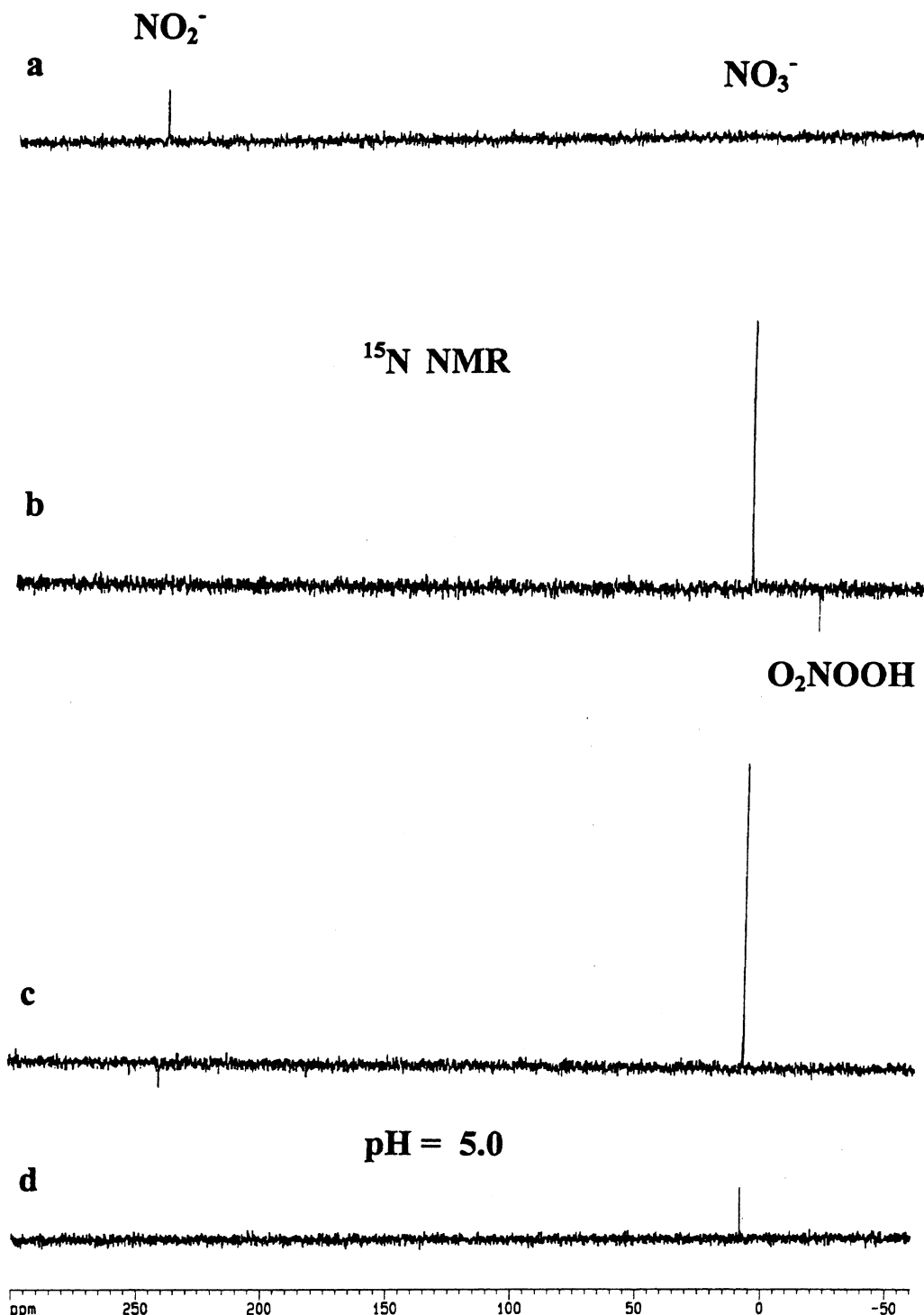


Figure 1. ^{15}N NMR spectra recorded during reaction of $\text{Na}^{15}\text{NO}_2$ with H_2O_2 and NaHCO_3 in $\text{H}_2\text{O}/\text{D}_2\text{O}$, taken with single scans (pulse angles 90°) (a) at pH 5.0 before adding and (b) 2 min, (c) 8 min, and (d) 30 min after adding of H_2O_2 to the solution.

provide estimates within “chemical accuracy” ($\pm 1\text{--}2 \text{ kcal mol}^{-1}$), as has also been demonstrated for O_2NOOH -related reactions.³⁹

ESR Measurements. ESR measurements were performed at ambient temperature on a Bruker ESP-300E spectrometer similarly as described.⁸ Solutions of 17 mM peroxyntic acid and 100 mM DMPO or POBN and of 170 mM peroxyntic acid and 1 M DMPO or POBN, respectively, in phosphate buffer were employed in a 0.4-mm quartz flat cell. Similar experiments were performed in the presence of 200 mM and 2 M concentrations of $[\text{C}_2^{13}]\text{DMSO}$ and $[\text{D}_6]\text{DMSO}$, respectively. Instrument settings (unless otherwise indicated): microwave frequency, 9.8 GHz; microwave power, 20

mW; sweep range, 100 G; sweep time, 4 min; modulation amplitude, 1 G. Spectral simulations were carried out with the WinSim program.⁴⁰

NMR Measurements. ^1H and ^{13}C NMR product analyses were performed on a Bruker DRX 500 spectrometer operating at 500 and 125.7 MHz, respectively. ^{13}C NMR spectra were acquired by collecting 16 transients. Spectra are referenced with respect to tetramethylsilane (TMS, $\delta = 0 \text{ ppm}$). Reaction of peroxyntic acid with $[\text{C}_2^{13}]\text{DMSO}$ was carried out as follows: Stock solutions of $[\text{C}_2^{13}]\text{DMSO}$ (100 mM) in H_3PO_4 (50 mM) and K_3PO_4 (50 mM), respectively, were freshly prepared each day. $[\text{C}_2^{13}]\text{DMSO}$ solutions

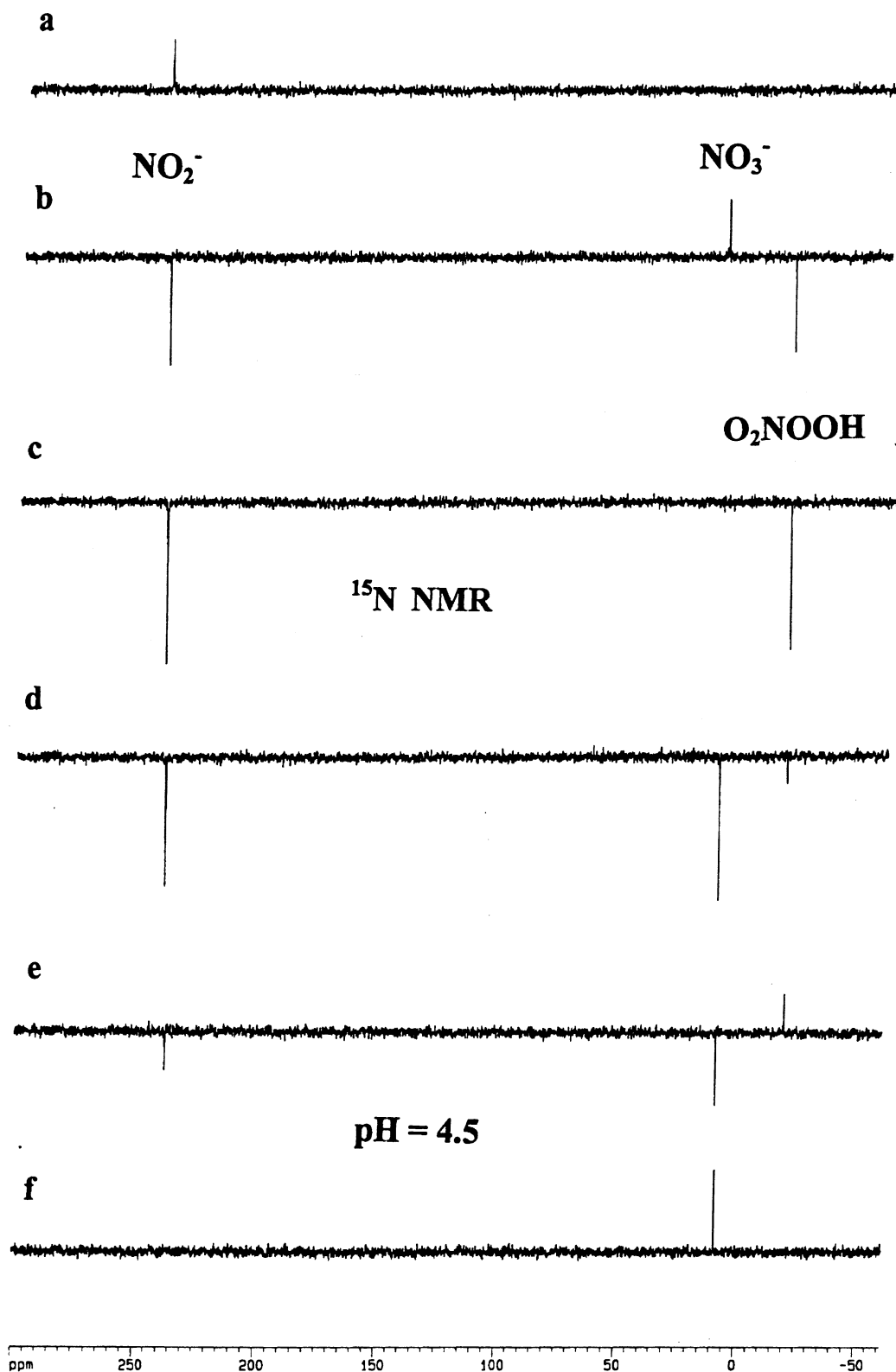


Figure 2. ^{15}N NMR spectra recorded during reaction of $\text{Na}^{15}\text{NO}_2$ with H_2O_2 and NaHCO_3 in $\text{H}_2\text{O}/\text{D}_2\text{O}$, taken with single scans (pulse angles 90°) (a) at pH 4.5 before adding and (b) 1 min, (c) 3 min, (d) 4 min, (e) 5 min, and (f) 15 min after adding of H_2O_2 to the solution.

of pH 1.75, 4.2, and 7, respectively, were prepared by mixing appropriate amounts of the stock solutions to phosphate buffer solutions of the desired pH. Aliquots of these mixtures were added under vortexing to solutions of freshly prepared peroxynitric acid to give a final concentration of 10 mM. After a reaction period of 90 min at 20°C D_2O was added (9:1 $\text{H}_2\text{O}/\text{D}_2\text{O}$) to the reaction

mixture and an aliquot of the resulting solution was transferred to 5-mm NMR tubes.

Results and Discussion

^{15}N NMR spectra taken after adding H_2O_2 to aqueous solutions of $\text{Na}^{15}\text{NO}_2$ in the presence of NaHCO_3 show a

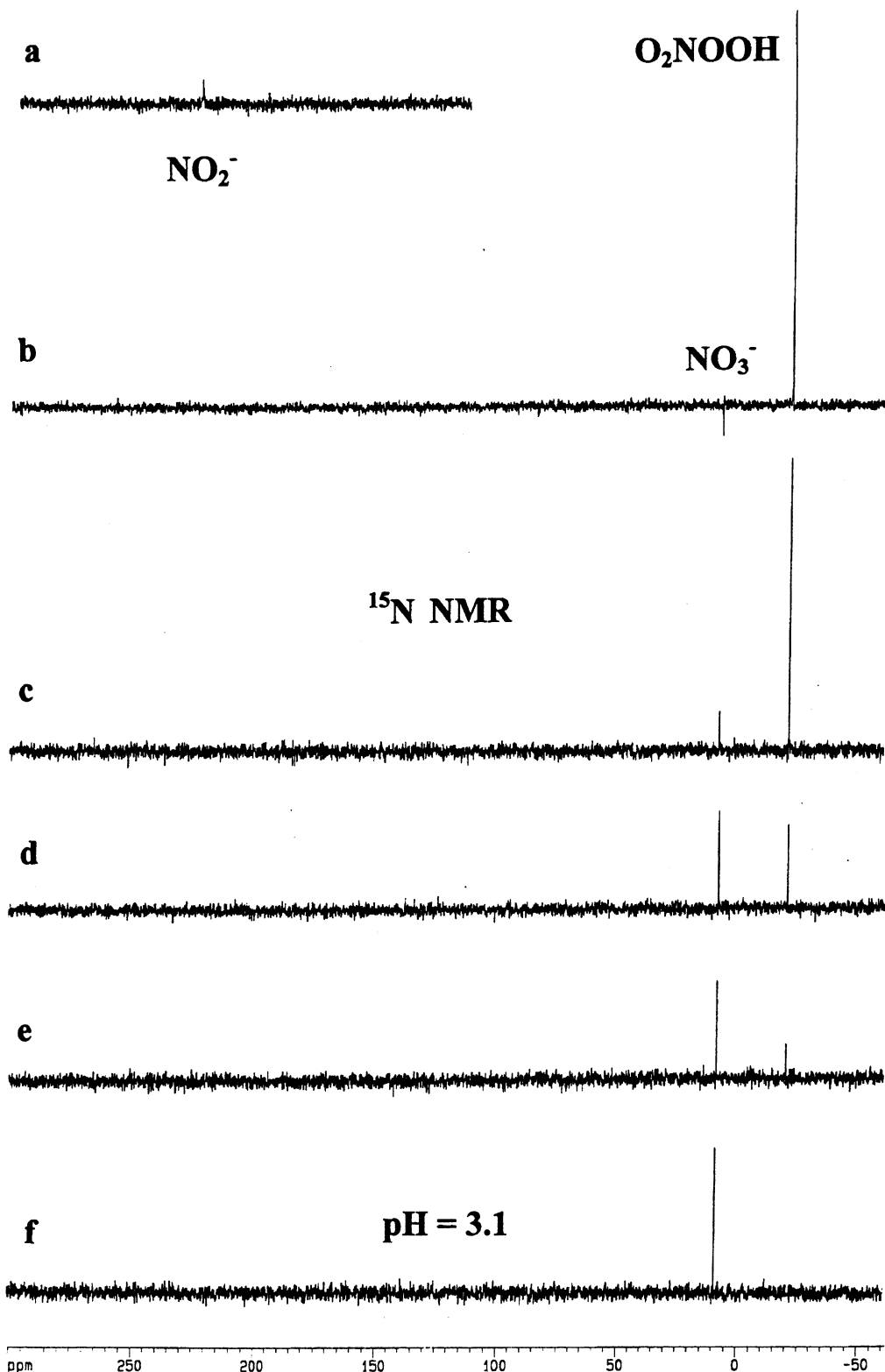


Figure 3. ^{15}N NMR spectra recorded during reaction of $\text{Na}^{15}\text{NO}_2$ with H_2O_2 and NaHCO_3 in $\text{H}_2\text{O}/\text{D}_2\text{O}$ at pH 4.3, taken with single scans (pulse angles 90°) (a) at pH 3.1 before adding and (b) 2 min, (c) 10 min, (d) 20 min, (e) 30 min, and (f) 120 min after adding of H_2O_2 to the solution.

puzzling variety of ^{15}N CIDNP effects, depending on the actual pH value and the elapsed time after mixing of the reactants. Typical spectra taken at pH 5.0, 4.5, and 3.1 are given in Figures 1–3; the assignment of the signals and details of the reaction conditions are listed in Table 1 and will be discussed in the following. A spectrum taken at pH

5.25 has already been published²⁶ and will also be included in the discussion. Spectra observed at pH 4.5 in the presence of Val-Tyr-Val and bovine albumin have also been described previously.²⁷

Prior to reaction, the ^{15}N NMR signal of NO_2^- is observed at $\delta = 240$ ppm; after complete reaction only that of NO_3^-

Table 1. ^{15}N CIDNP Effects Observed during Reaction of $\text{Na}^{15}\text{NO}_2$ with H_2O_2 ^a

pH	<i>t</i> (min) ^b	assgnt	δ (ppm) ^c	CIDNP ^d
5.25 ²⁷	90	NO_2^-	240	$\text{N} \rightarrow 0$
		NO_3^-	9	$0 \rightarrow \text{A} \rightarrow \text{N}$
5.0 (Fig 1)	30	NO_2^-	240	$\text{N} \rightarrow 0$
		NO_3^-	9	$0 \rightarrow \text{A} \rightarrow \text{N}$
		O_2NOOH	-18	$0 \rightarrow \text{E} \rightarrow 0$
4.5 (Fig 2)	10	NO_2^-	240	$\text{N} \rightarrow \text{E} \rightarrow 0$
		NO_3^-	9	$0 \rightarrow \text{A} \rightarrow \text{E} \rightarrow \text{N}$
		O_2NOOH	-18	$0 \rightarrow \text{E} \rightarrow \text{A} \rightarrow 0$
3.1 (Fig 3)	90	NO_2^-	240	$\text{N} \rightarrow 0$
		NO_3^-	8	$0 \rightarrow \text{E} \rightarrow \text{N}$
		O_2NOOH	-18	$0 \rightarrow \text{A} \rightarrow 0$

^a 1 M H_2O_2 , 0.05 M $\text{Na}^{15}\text{NO}_2$, 0.05 M NaHCO_3 in $\text{H}_2\text{O}/\text{D}_2\text{O}$ (9:1) with 0.5 M potassium phosphate, $T = 295$ K. ^b Total reaction time from mixing of the reactants until completion of the reaction. ^c δ in ppm relative to [^{15}N]nitrobenzene, positive δ values downfield. ^d E, emission; A, enhanced absorption; N, no CIDNP effect; 0, no ^{15}N NMR signal.

at $\delta = 8$ ppm can be detected; see Figures 1a,d, 2a,f, and 3a,f. Thus, nitrate is the only stable reaction product in this system, as expected. The ^{15}N NMR signals of NO_2^- and NO_3^- exhibit a variety of ^{15}N CIDNP effects during the course of the reaction. At $\text{pH} < 5$, an additional, transient signal is observed at $\delta = -18$ ppm, appearing in emission or enhanced absorption depending on the progress of the reaction. The chemical shift identifies this signal to be due to peroxynitric acid.⁶

At $\text{pH} 5.25$, the reaction is finished after about 90 min. Due to the low overall reaction rate peroxynitric acid is not detectable at this pH .²⁶ The intensity of the ^{15}N NMR signal of NO_2^- decreases during the reaction without showing any ^{15}N CIDNP effect. The ^{15}N NMR signal of NO_3^- shows enhanced absorption. These features have been explained by decomposition of the very short-lived peroxynitrite- CO_2 adduct with formation of a radical pair [NO_2^\bullet , $\text{CO}_3^{\bullet-}$]⁵, according to eqs 12, 14, and 15); see Scheme 2.^{26, 27, 29}

At $\text{pH} 5.0$, the reaction is completed after 30 min. In addition to the effects observed at $\text{pH} 5.25$, the ^{15}N NMR signal of O_2NOOH can now be monitored, appearing in emission during the first 5 min of the reaction (Figure 1b).

At $\text{pH} 4.5$, the total reaction time is further reduced to less than 10 min. The ^{15}N NMR signal of NO_3^- shows enhanced absorption at the beginning of the reaction but changes to emission after about 2 min (Figure 2b-d). The ^{15}N NMR signal of O_2NOOH shows emission at the

beginning of the reaction (Figure 2b) and enhanced absorption later in the course of the reaction (Figure 2e). The signal of NO_2^- appears in emission at all times. The pH value declines during the reaction to $\text{pH} 4.0$ after the reaction which did not allow to determine the exact pH value at which the reaction time reaches an expected minimum (see below).

At $\text{pH} 3.1$, the reaction rate is decreased again to an overall reaction time of about 90 min. The ^{15}N NMR signal of NO_3^- shows emission at the beginning and no effect later (> 5 min); see Figure 3. The ^{15}N NMR signal of O_2NOOH shows enhanced absorption from the beginning of the reaction until complete decay. A half-life of about 20 min for the decay of O_2NOOH is deduced from the time dependency of the ^{15}N NMR signal. This value is in reasonable agreement with the half-life (30 min) for decomposition of O_2NOOH as reported in the literature.⁶ The decay rate does not change by lowering the pH value further. When preformed peroxynitric acid is utilized, identical decay rates are observed.

The overall reaction times as well as the ^{15}N CIDNP spectra taken during reaction of $^{15}\text{NO}_2^-$ with H_2O_2 are governed by the rates of formation and decay of peroxynitrous acid, the peroxynitrite- CO_2 adduct, and peroxynitric acid. It can be expected that the properties of the latter are not influenced by the presence of CO_2 .⁴¹ The individual reactions exhibit different pH dependencies, the possible influence of which on the NMR spectra will be discussed first. By doing so, it should be kept in mind that reactions which occur within less than 1 min after mixing of the reactants cannot be observed for practical reasons. Also, weak CIDNP effects might not be observed when the reaction rates are low. The ^{15}N CIDNP spectra shown in Figures 1-3 were selected because they reflect most clearly the (radical) reactions which dominate the system in the pH range 3-5. Further, it should be noticed that CIDNP effects observed in an individual NMR spectrum are mainly created by radical reactions belonging to the same reaction sequence.

The rate of formation of peroxynitrous acid increases with decreasing pH value.⁴²⁻⁴⁵ At $\text{pH} \geq 4.6$ this reaction needs more than 1 min under the applied reaction conditions, whereas the formation of the peroxynitrite- CO_2 adduct (eq 14) occurs within less than 1 s ($k_{14} = 3 \times 10^4 \text{ M}^{-1} \text{ s}^{-1}$).¹⁹ This fact allows the observation of the enhanced absorption in NO_3^- , built up during homolysis of the peroxynitrite- CO_2 adduct at $\text{pH} 4.5, 5.0$, and 5.25 (eq 15), which occurs within 1 ms after its formation ($k_{15} \geq 6.7 \times 10^5 \text{ M}^{-1} \text{ s}^{-1}$);⁸ see Figures 1b,c and 2b. Because of the short lifetime of the peroxynitrite- CO_2 adduct, a ^{15}N CIDNP effect which might be built up in this intermediate cannot be observed. At $\text{pH} 3.1$, the formation and decay of the peroxynitrite- CO_2 adduct is finished before the first spectrum can be taken, preventing any monitoring of enhanced absorption in the ^{15}N NMR signal of NO_3^- . The formation of peroxynitric acid via

- (38) Frisch, M. J.; Trucks, G. W.; Schlegel, H. B.; Scuseria, G. E.; Robb, A. A.; Cheeseman, J. R.; Zakrzewski, V. G.; Montgomery, J. A.; Stratmann, R. E.; Burant, J. C.; Dapprich, S.; Millam, J. M.; Daniels, A. D.; Kudin, K. N.; Strain, M. C.; Farkas, O.; Tomasi, J.; Barone, V.; Cossi, M.; Cammi, R.; Mennucci, B.; Pomelli, C.; Adamo, C.; Clifford, S.; Ochterski, J.; Petersson, G. A.; Ayala, P. Y.; Cui, Q.; Morokuma, K.; Malick, D. K.; Rabuck, A. D.; Raghavachari, K.; Foresman, J. B.; Cioslowski, J.; Ortiz, J. V.; Stefanov, B. B.; Liu, G.; Liashenko, A.; Piskorz, P.; Komaromi, I.; Gomperts, R.; Martin, R. L.; Fox, D. J.; Keith, T.; Al-Laham, M.-A.; Peng, C. Y.; Nanayakkara, A.; Gonzalez, C.; Challacombe, M.; Gill, P. M. W.; Johnson, B. G.; Chen, W.; Wong, M. W.; Andres, J. L.; Head-Gordon, M.; Replogle, E. S.; Pople, J. A. *Gaussian 98W*, revision A.9; Gaussian: Pittsburgh, PA, 2000.
- (39) Miller, C. E.; Lynton, J. I.; Keevil, D. M.; Francisco, J. S. *J. Phys. Chem. A* **1999**, *103*, 11451-11459.
- (40) Duling, D. R. *WinSim*; Laboratory of Molecular Biophysics, NIEHS, NIH: Research Triangle Park, NC. See: Duling, D. R. *J. Magn. Reson. B* **1994**, *105*, 105-110.

- (41) Goldstein, S.; Lind, J.; Merenyi, G. *J. Chem. Soc., Dalton Trans.* **2002**, 808-810.
- (42) Anbar, M.; Taube, H. *J. Am. Chem. Soc.* **1984**, *76*, 6243-6247.
- (43) Benton, D. J.; Moore, P. J. *J. Chem. Soc. A* **1970**, 3179-3182.
- (44) Saha, A.; Goldstein, S.; Cabelli, D.; Czapski, G. *Free Radical Biol. Med.* **1998**, *24*, 653-659.
- (45) Goldstein, S.; Czapski, G. *Inorg. Chem.* **1997**, *36*, 4156-4162.

Table 2. Quantum-Chemically Calculated Gibbs Energies and Aqueous Solvation Energies

entry	reaction ^a	$\Delta_r G$ (kcal mol ⁻¹)		
		$\Delta_r G_g^b$	$\Delta_r G_{\text{solv}}^c$	$\Delta_r G_{\text{aq}}^d$
1	$\text{O}_2\text{NOOH} + \text{NO}_2^- \rightarrow \text{O}_2\text{NOOH}^{\cdot-} + \text{NO}_2^{\cdot}$	20.7	14.2	34.9
2	$\text{O}_2\text{NOOH} + \text{O}_2^{\cdot-} \rightarrow \text{O}_2\text{NOOH}^{\cdot-} + \text{O}_2$	-20.2	27.4	7.2
3	$\text{O}_2\text{NOOH} + \text{O}_2\text{NOO}^- \rightarrow \text{O}_2\text{NOOH}^{\cdot-} + \text{NO}_2^{\cdot} + \text{O}_2$	5.5	10.7	16.2
4	$\text{O}_2\text{NOOH} + \text{ONOO}^- \rightarrow \text{O}_2\text{NOOH}^{\cdot-} + \cdot\text{NO} + \text{O}_2$	3.7	16.9	20.5
5	$\text{O}_2\text{NOOH}^{\cdot-} \rightarrow \text{HO}^{\cdot} + \text{NO}_3^-$	-31.4	-6.0	-37.4
6	$\text{O}_2\text{NOOH}^{\cdot-} \rightarrow \text{HO}^- + \text{NO}_3^{\cdot}$	20.6	-46.7	-26.1
7	$\text{O}_2\text{NOOH}^{\cdot-} \rightarrow \text{HOO}^{\cdot} + \text{NO}_2^-$	-9.2	-13.2	-22.4
8	$\text{O}_2\text{NOOH}^{\cdot-} \rightarrow \text{HOO}^- + \text{NO}_2^{\cdot}$	17.1	-28.0	-10.9

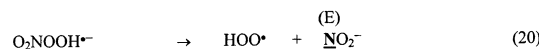
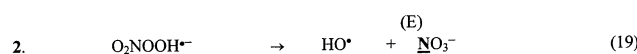
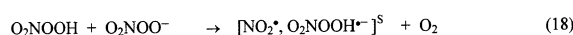
^a Thermodynamic properties were calculated using the complete basis set (CBS-Q) methodology. ^b Gas-phase data. ^c Solvation corrections from (U)HF/6-31+G(d)//CBS-Q single point calculations with the PCM-UAHF solvation model for water.⁵¹ ^d $\Delta_r G_{\text{aq}} = \Delta_r G_g + \Delta_r G_{\text{solv}}$.

Scheme 3. ¹⁵N CIDNP Effects during Formation and Decay of Peroxynitric Acid

Formation:



Decay:



reaction 1 is diffusion-controlled ($k_1 = 1.8 \times 10^9 \text{ M}^{-1} \text{ s}^{-1}$),¹⁶ therefore strongly correlated with the formation of peroxynitrous acid and the peroxynitrite-CO₂ adduct. The emission observed in the ¹⁵N NMR signal of peroxynitric acid appears simultaneously with the enhanced absorption in the ¹⁵N NMR signal of NO₃⁻ (Figures 1b and 2b). These effects are therefore assigned to a reaction correlated with the formation of peroxynitric acid via reaction 1. In contrast to this, the decay of peroxynitric acid is retarded and determines the overall reaction rate and thus the ¹⁵N CIDNP spectra observed later in the course of the reaction, especially at low pH values. The ¹⁵N CIDNP spectra observed under these conditions (Figures 2c–e and 3) are consequently attributed to reactions of peroxynitric acid. Reaction sequences involving peroxynitric acid which are capable to explain the observed ¹⁵N CIDNP effects are displayed in Scheme 3 and will now be discussed in detail. For supporting the feasibility of some the discussed reactions, quantum-chemical calculations have been performed. The results are collected in Table 2. The first process to be considered is the homolytic decay already described in the literature (eq -1); the second one is a specification of the oxidative properties of peroxynitric acid (eqs 9 and 10).

The emission observed in the ¹⁵N NMR signal of O₂NOOH is explained by the formation of peroxynitric according to reaction 1.²⁷ NO₂[·] is formed by homolysis of peroxynitrite and/or the peroxynitrite-CO₂ adduct (eqs 13 and 15), and HOO[·] stems from reaction of HO[·] and/or CO₃^{·-} with H₂O₂ (eqs 16 and 17). The diffusion-controlled encounter of NO₂[·] and HOO[·] radicals generates F pairs, [NO₂[·], HOO[·]]^F, leading to emission in the ¹⁵N NMR signal of the recombination (c) product O₂NOOH (Scheme 1) because of $g(\text{HOO}^{\cdot}) > g(\text{NO}_2^{\cdot})$.^{33,46} This type of emission can only be observed at pH ≤ 4.8, i.e., the pK_a of HOO[·], because radical pairs [NO₂[·],

O₂^{·-}]^F do not evolve CIDNP. On the other hand, the emission might also be, at least in part, an escape (e) type polarization built up in geminate radical pairs (S pairs) [NO₂[·], CO₃^{·-}]^S and transferred into peroxynitric acid via reaction 1. Contrary to the F pair process however, such a pathway would also lead to CIDNP at pH > 4.8. As the observed polarization is weak at pH 5.0 and can no longer be detected at pH 5.25, an F pair mechanism as displayed in Scheme 3 (eq 1) is more likely. However, an unequivocal decision in favor of the latter mechanism cannot be made as the reaction rate is low at higher pH values, which also might explain the absence of the ¹⁵N CIDNP effect in peroxynitric acid.

The enhanced absorption observed in the ¹⁵N NMR signal of O₂NOOH (see Figures 2e and 3b–e) is of c type and arises from radical pairs [NO₂[·], HOO[·]]^S formed by homolysis-cage recombination of peroxynitric acid (eq -1). This CIDNP effect again can only be built up effectively at pH ≤ 4.8, below the pK_a of HOO[·]. Because of this, any occurrence of reaction -4 cannot be proven by CIDNP. As reaction 5 does not lead to ¹⁵N CIDNP either, homolysis of peroxynitric acid is expected to be CIDNP inactive at higher pH values, in accord with the experimental observations; compare Figure 1.

Of special interest is the emission-type polarization in the ¹⁵N NMR signal of NO₃⁻ observed at pH 4.5 and pH 3.1 (Figure 3b). This feature cannot be explained by the foregoing discussed reactions. At pH 4.5, the emission signal appears in combination with emission signals of NO₂⁻ and O₂NOOH without any other signal showing enhanced absorption; see Figure 2d. It follows from the radical pair model of CIDNP that e type polarizations are always created in combination with c type polarizations. The latter are about 1 order of magnitude stronger than those of e type because of nuclear relaxation in the radicals.^{29,50} Hence, if the nuclear relaxation times in the reaction products are similar, which should be the case here, CIDNP signals of c products are more intense than those of e products. Therefore, we have to conclude that all three emission signals are due to c

(46) Landolt-Börnstein, *New Series, Group II, Magnetic Properties of Free Radicals*, Vols. II/17a–h; Fischer, H., Ed.; Springer-Verlag: Berlin, 1987–1990.

(47) Stanbury, D. M.; deMaine, M. M.; Goodloe, G. *J. Am. Chem. Soc.* **1989**, *111*, 5496–5498.

(48) Thomas, K. J. *Adv. Radiat. Chem.* **1969**, *1*, 103–198.

(49) Schwartz, A.; White, W. H. *Adv. Environ. Sci. Technol.* **1983**, *12*, 1–116.

(50) Lehnicg, M.; Fischer, H. Z. *Naturforsch.* **1972**, *27A*, 1300–1307.

products from radical reactions which contribute to a significant extent in a small pH region around pH 4.6 only. Whereas the emission-type polarization in peroxynitric acid is easily explained by reaction 1, we propose that the polarizations in NO_2^- and NO_3^- are built up in radical pairs $[\text{NO}_2^\bullet, \text{O}_2\text{NOOH}^{\bullet-}]^{\text{S}}$, deriving from diffusive encounters of peroxynitric acid and peroxynitrate anion, and subsequent one-electron transfer between them (eq 18). That is, peroxynitric acid is assumed to oxidize its own anion. The initial oxidation product of peroxynitrate, $\text{O}_2\text{NOO}^\bullet$, should be highly unstable and expected to decay instantaneously to NO_2^\bullet and O_2 . Hence, NO_2^\bullet is produced in the solvent cage together with the reduction product, the radical anion of peroxynitric acid, $\text{O}_2\text{NOOH}^{\bullet-}$, both forming a singlet radical pair. Radical pairs $[\text{NO}_2^\bullet, \text{O}_2\text{NOOH}^{\bullet-}]^{\text{S}}$ would produce c type effects in the ^{15}N NMR signals of NO_2^- as well as NO_3^- by decomposition of $\text{O}_2\text{NOOH}^{\bullet-}$ via reactions 19 and 20. More general, the hitherto unknown $\text{O}_2\text{NOOH}^{\bullet-}$ might not only be produced via reaction 18 but by reaction of O_2NOOH with any other strongly sufficient reductant in the system (see below).

Although $\text{O}_2\text{NOOH}^{\bullet-}$ is intuitively expected to be a short-lived species, especially in aqueous solution, the hypothesis of its intermediacy is nevertheless supported by quantum-chemical calculations at the CBS-Q level of theory in combination with the PCM solvation model (Table 2).

On this level of theory, $\text{O}_2\text{NOOH}^{\bullet-}$ is found to be a stable, intramolecularly hydrogen-bonded structure in the gas phase, with the unpaired electron residing in a π^* -type orbital delocalized over the O_2NO moiety (see Supporting Information, Figure S1). The computations predict solvent-corrected Gibbs energies of $\Delta_r G_{\text{aq}} = -37.4$ kcal mol $^{-1}$ for the formation of NO_3^- and of -22.4 kcal mol $^{-1}$ for the formation of NO_2^- from this species (Table 2, entries 5 and 7).

Peroxynitric acid is known to be a strong oxidizing agent; hence, the formation of its radical anion might be caused by any potential one-electron reductant present in the solution at medium acidic pH values. It has been reported that the decomposition of O_2HOOH is accelerated by addition of nitrite (eq 9).¹² However, our quantum-chemical calculations predict that the reaction with NO_2^- as electron donor (eq 21) is energetically highly disfavored by $\Delta_r G_{\text{aq}} = 34.9$ kcal mol $^{-1}$ (Table 2, entry 1).

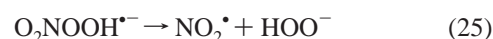
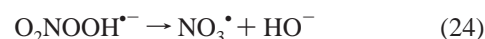


Another reducing agent which might be capable of transferring an electron onto O_2NOOH is superoxide (eq 22). In fact, as an electron transfer between $\text{O}_2^{\bullet-}$ and peroxynitric acid appears to be the least endergonic reaction ($\Delta_r G_{\text{aq}} = 7.2$ kcal mol $^{-1}$; Table 2, entry 2), reaction 22 may be a likely source for the putative peroxynitric acid radical anion. On the other hand, reaction 22 should be kinetically unimportant because of the low stationary concentration of $\text{O}_2^{\bullet-}$ under the applied experimental conditions. More probable seems to be an electron transfer between O_2NOOH and ONOO^- (eq 23; $\Delta_r G_{\text{aq}} = 20.5$ kcal mol $^{-1}$; Table 2, entry 4) or between O_2NOOH and O_2NOO^- (eq 18; $\Delta_r G_{\text{aq}} = 16.2$ kcal

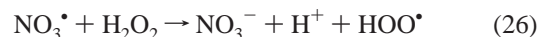
mol $^{-1}$; Table 2, entry 3). On the basis of these data, we propose that reaction 18 is the likely source of the putative peroxynitric acid radical ion. In accord with the experimental observations, this reaction is predicted to be of importance only in a small pH range, around the pK_a value (5.8) of peroxynitric acid where both the O_2NOOH and the O_2NOO^- concentrations are high.



Unimolecular homolytic decomposition of $\text{O}_2\text{NOOH}^{\bullet-}$ can occur by O–O and O–N bond cleavage, reactions 19, 20, 24, and 25. Whereas in the gas phase only reactions 19 and 20 are energetically downhill, all four pathways are predicted to be thermochemically feasible in aqueous solution (Table 2, entries 5–8). Indications for the preferred reaction path(s) were sought by computation of the corresponding transition structures followed by intrinsic reaction coordinate (IRC)⁵² calculations at the same level of theory. Unfortunately, the CBS-Q method failed to locate the transition structures; therefore, the PCM-(U)HF/6-31+G(d)//UMP2/6-31+G(d,p) procedure was employed (see Supporting Information, Table S1, entries 1–6).



The transition structures for dissociation of the $\text{O}_2\text{N}-\text{OOH}^{\bullet-}$ and the $\text{O}_2\text{NO}-\text{OH}^{\bullet-}$ bonds are calculated to be $\Delta G_{\text{aq}}^\ddagger = 7.1$ and 16.1 kcal mol $^{-1}$, respectively, above the energy level of the $\text{ONOOH}^{\bullet-}$ radical (Table S1, entries 1 and 4).⁵³ The IRC calculations (data not show) predict the formation of NO_2^- and HOO^\bullet on cleavage of the $\text{O}_2\text{N}-\text{OOH}^{\bullet-}$ bond (eq 20) and of NO_3^- and HO^\bullet on $\text{O}_2\text{NO}-\text{OH}^{\bullet-}$ bond cleavage (eq 19) with $\Delta_r G_{\text{aq}} = -22.4$ and -37.4 kcal mol $^{-1}$, respectively (Table 2, entries 5 and 7). The ^{15}N CIDNP effects might also be explained, at least in part, by radical reactions involving NO_3^\bullet instead of $\text{O}_2\text{NOOH}^{\bullet-}$. Although fragmentation into HO^- and NO_3^\bullet (eq 24) also turns out to be thermochemically feasible in aqueous solution (Table 2, entry 6), the IRC calculations, however, disapprove homolysis into NO_3^\bullet and HO^- . Further, NO_3^\bullet reacts rapidly with H_2O_2 (eq 26; $k_{26} = 1.9 \times 10^6$ M $^{-1}$ s $^{-1.54}$); thus, formation of radical pairs by diffusive encounters should largely be suppressed. In addition, nitrite is not a product from reactions with NO_3^\bullet .

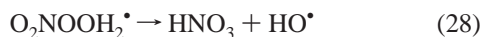
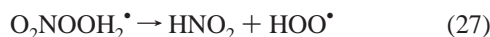


One might argue that in acidic solution $\text{O}_2\text{NOOH}^{\bullet-}$ would rapidly be protonated to give the transient $\text{O}_2\text{NOOH}_2^\bullet$ radical, which then might decompose to HOO^\bullet and HNO_2 (eq 27) and/or to HO^\bullet and HNO_3 (eq 28), respectively. This cannot

(51) Barone, V.; Cossi, M.; Tomasi, J. *J. Chem. Phys.* **1997**, *107*, 3210–3221.

(52) Gonzales, C.; Schlegel, H. B. *J. Chem. Phys.* **1989**, *90*, 2154–2161.

be excluded; however, the calculations predict that protonation of $\text{O}_2\text{NOOH}^{\bullet-}$ even slightly increases the lifetime of this species, because the transition state energies of these reactions (Table S1, entries 7–12) are calculated to be increased to $\Delta G_{\text{aq}}^\ddagger = 12.5$ and $19.6 \text{ kcal mol}^{-1}$, respectively.



Radical pairs $[\text{NO}_2^{\bullet}, \text{O}_2\text{NOOH}^{\bullet-}]^{\text{S}}$ lead to emission in products such as NO_3^- and NO_2^- if $g(\text{O}_2\text{NOOH}^{\bullet-}) > g(\text{NO}_2^{\bullet})$; see Scheme 1. The g -value of NO_2^{\bullet} is 2.000,^{46,55} but the g -value of the proposed $\text{O}_2\text{NOOH}^{\bullet-}$ is not known. However, $g > 2$ has been reported for radical anions similar to $\text{O}_2\text{NOOH}^{\bullet-}$.⁴⁶ Thus, the assumption $g(\text{O}_2\text{NOOH}^{\bullet-}) > g(\text{NO}_2^{\bullet})$ is reasonable.

Koppenol and co-workers suggested the existence of $\text{O}_2\text{NOOH}^{\bullet-}$ during reaction of HO^{\bullet} with ONOO^- .⁵⁶ Goldstein et al. reported that the reduction of O_2NOOH might give HO^{\bullet} radicals (eq 10).¹³ The latter authors did not consider the formation of $\text{O}_2\text{NOOH}^{\bullet-}$ as a reactive intermediate.

As reaction 19 appears to be energetically favorable, hydroxyl radicals are expected to be released on decomposition of $\text{O}_2\text{NOOH}^{\bullet-}$. Unfortunately, due to the inherent strong spin-orbit coupling of HO^{\bullet} radicals their intermediacy cannot be detected by CIDNP. To provide evidence for HO^{\bullet} radical formation on O_2NOOH decomposition, the reaction of O_2NOOH with DMSO was investigated by ^{13}C NMR spectrometry. Reaction of O_2NOOH with $^{13}\text{C}_2$ DMSO should allow a distinction between “directly” oxidizing O_2NOOH and “indirect” oxidation via HO^{\bullet} . As a strong two-electron oxidant O_2NOOH is expected to oxidize DMSO to dimethyl sulfone:⁴⁵



On the other hand, oxidation of DMSO by hydroxyl radicals is known to yield methanesulfinic acid, $\text{CH}_3\text{S}(\text{O})\text{OH}$, which is regarded to be a specific product from attack of HO^{\bullet} :⁵⁷



In an oxidizing environment, methanesulfinic acid is rapidly oxidized to methanesulfonic acid.⁵⁸ This oxidation is likely

(53) At first sight, these barriers seem to be fairly high; however, they should only be regarded as indicators for the short lifetime of $\text{ONOOH}^{\bullet-}$ and the relative order of the two bond breaking processes, because it has been found that the (UMP2/6-31+G(d,p) methods tends to overestimate activation barriers on the average by 5–6 kcal mol⁻¹; see: Lynch, B. J.; Truhlar, D. G. *J. Phys. Chem. A* **2001**, *105*, 2936–2941.

(54) Katsumura, J.; Jiang, P. Y.; Nagaishi, R.; Oishu, T.; Ishigure, K.; Yoshida, Y. *J. Phys. Chem.* **1991**, *95*, 4435–4439.

(55) Morton, J. R.; Preston, K. F.; Strach, S. J. *J. Phys. Chem.* **1979**, *83*, 533–535.

(56) Kissner, R.; Nauser, Th.; Bugnon, P.; Lye, P. G.; Koppenol, W. H. *Chem. Res. Toxicol.* **1997**, *10*, 1285–1292.

(57) Veltwisch, D.; Janata, E.; Asmus, K.-D. *J. Chem. Soc., Perkin Trans. 2* **1980**, 146–153.

(58) Richeson, C. E.; Mulder, Bowry, P. V. W.; Ingold, K. U. *J. Am. Chem. Soc.* **1998**, *120*, 7211–7219.

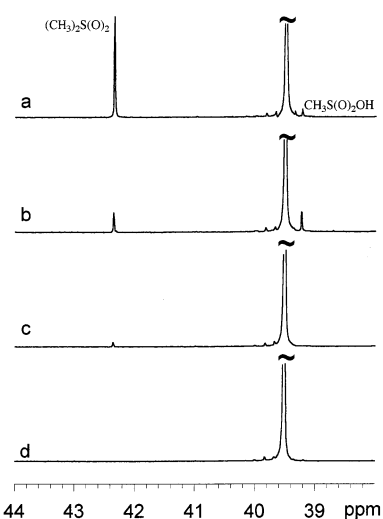
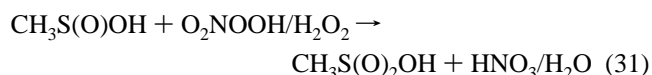


Figure 4. 125.7 MHz ^{13}C NMR spectra recorded after reaction of O_2NOOH (10 mM) with $^{13}\text{C}_2$ DMSO (100 mM) in $\text{H}_2\text{O}/\text{D}_2\text{O}$ at (a) pH 1.75, (b) pH 4.2, and (c) pH 7, respectively. (d) shows the ^{13}C NMR spectrum of pure $^{13}\text{C}_2$ DMSO at pH 7. The intensities of the spectra were normalized with respect to the $^{13}\text{C}_2$ DMSO resonance at 39.5 ppm. The cutoff of the $^{13}\text{C}_2$ DMSO signal is at about 8% of its full intensity.

to be mediated by both O_2NOOH and H_2O_2 :⁵⁹



Typical ^{13}C NMR spectra are shown in Figure 4; corresponding ^1H NMR spectra are provided as Supporting Information (Figure S2). In fact, the “two-electron product” dimethyl sulfone and the “ HO^{\bullet} product” methanesulfonic acid were identified by ^1H and ^{13}C NMR spectrometry when peroxyntic acid was decomposed in the presence of $^{13}\text{C}_2$ -DMSO at pH 4.2. At this pH, the yield of methanesulfonic acid ($\delta = 39.2$) is approximately twice the yield of methyl sulfone ($\delta = 42.3$ ppm). Figure 4d proves that neither dimethyl sulfone nor methanesulfonic acid are contaminants in the applied $^{13}\text{C}_2$ DMSO. The formation of methanesulfonic acid is reduced at lower pH while the yield of dimethyl sulfone is strongly increased (Figure 4a).

With increasing pH, the yields of both products are diminished, and at pH 7 methanesulfonic acid can no longer be detected (Figure 4c). Such a behavior is just what has to be expected if hydroxyl radicals are being produced via reaction 19. Thus, product formation indicates that hydroxyl radical release is governed by the $\text{p}K_{\text{a}}$ of O_2NOOH , in full agreement with the above CIDNP experiments. At higher gain, the ^{13}C NMR spectra reveal the presence of a variety of minor products (see Supporting Information, Figure S3). At pH 1.7, additional signals of similar intensity of unidentified products at $\delta = 93.4$, 82.7, and 65.8 and a very weak peak of methanol at $\delta = 49.8$ ppm are detected. The methanol peak is about 3-fold increased at pH 4.2, whereas the other signals are diminished. From integration of the ^1H NMR signals the overall conversion of $^{13}\text{C}_2$ DMSO is

(59) An anonymous reviewer suggested that NO_2^{\bullet} may additionally react with $\text{CH}_3\text{S}(\text{O})\text{OH}$ to yield $^{\bullet}\text{NO}$ and $\text{CH}_3\text{S}(\text{O})_2\text{OH}$, respectively. This reaction cannot be ruled out.

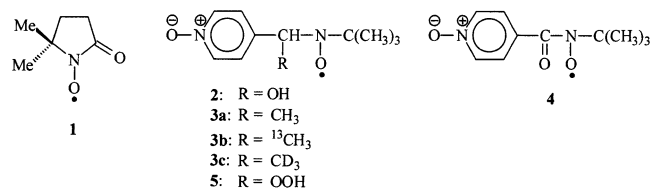
estimated to about 8 mol %. Noteworthy, now a new, rather strong signal (approximately 25% of the intensity of the dimethyl sulfone peak) is observed at $\delta = 61.2$ ppm. This peak was identified as being due to nitromethane by “spiking” with authentic material. Nitromethane is reasonably formed from recombination of methyl radicals and NO_2^\bullet . Methanol is a known product from initial reaction of CH_3^\bullet with oxygen but might also derive from hydrolysis of methyl nitrite, the other possible recombination product of CH_3^\bullet and NO_2^\bullet . Thus, methanol and nitromethane strongly indicate the intermediacy of methyl radicals, as is required by reaction 30, further supporting the release of hydroxyl radicals and NO_2^\bullet from peroxynitric acid at pH 4–5. In accord with the discussed pH dependence of HO^\bullet production, none of the minor products can be detected at pH 7. This fact further suggests that peroxynitrate anion does not react with DMSO other than by two-electron oxidation at sulfur to give dimethyl sulfone.

As mentioned in the Introduction, it is widely accepted that during decomposition of peroxynitrous acid, ONO_2H , free HO^\bullet and NO_2^\bullet radicals are released with a yield of about $28 \pm 2\%$.^{14,17} Hydroxyl radical generation from peroxynitrous acid has been probed with DMSO previously, revealing the formation of dimethyl sulfone and methanesulfonic acid.⁵⁸ For comparison purposes, we reinvestigated by ^1H and ^{13}C NMR spectrometry the reaction of preformed ONO_2H with [$^{13}\text{C}_2$]DMSO under similar conditions as applied in the peroxynitric acid experiments (Supporting Information, Figure S4). At pH 4.0 [$^{13}\text{C}_2$]DMSO is converted to about 7% to yield five major products (^{13}C NMR shifts), methanesulfonic acid (39.2), dimethyl sulfone (42.3), methanol (49.8), nitromethane (61.2), and an unidentified one at 82.7 ppm, in an approximative molar ratio of 6.6:2.2:2.0:1.0:1.0, respectively. Thus, the product spectrum from peroxynitrous acid is very similar to that from peroxynitric acid in this pH range; however, the fraction of released HO^\bullet appears to be higher.

To gain further evidence for the generation of HO^\bullet radicals from peroxynitric acid, ESR spectra were taken during decomposition of preformed O_2NOOH in the presence of the spin trap compounds DMPO (5,5-dimethylpyrrolidine-1-oxide) and POBN [α -(4-pyridyl-1-oxide)-*N-tert*-butylnitron], respectively, both in the absence and presence of unlabeled and isotopically labeled ($^{13}\text{C}_2$, D_6) DMSO.

The experiments with DMPO were not conclusive with regard to the trapping of HO^\bullet or other possible O_2NOOH -derived radicals. Neither the HO^\bullet adduct of DMPO nor expected CH_3^\bullet adduct in the presence of DMSO (eq 30) could be detected. Therefore, ESR spectra and spectroscopic data are only provided as Supporting Information (Figures S5–S7, Table S2). Briefly, at pH 4.5 and in the absence of DMSO, the major component of the composite spectrum (Figure S5) was identified as the known carbonyl derivative of DMPO (**1**) [$a(\text{N}) = 7.26$, $a(\text{CH}_2) = 4.02$ G]. This nitroxide radical is a common, rather unspecific product from DMPO under oxidative conditions⁶⁰ and reflects the high oxidative power of O_2NOOH .⁶¹ In the presence of DMSO a strong, moderately persistent (half-life ca. 15 min) three-line spec-

trum of an yet unidentified radical (X_1) with $a(\text{N}) = 12.72$ G and unresolved, small splittings (≤ 0.8 G) was initially observed at pH 4.5 (some **1** was also detected) (Figure S6). Noteworthy, a very similar three-line spectrum was observed with POBN in the presence of DMSO (see below). At pH 1.9, the initial, composite spectrum indicated the presence of radicals **1** and X_1 and an unknown, longer-lived nitroxide (X_2) showing an additional, small nitrogen splitting [$a(\text{N}) = 14.42$, $a(\text{N}) = 1.27$ G] (Figure S7). The latter spectrum was also observed in the absence of DMSO (data not shown), thus merely indicating nitrogenation of DMPO by peroxynitric acid.



Application of the spin trap compound POBN provided more clear-cut results. At 17 mM O_2NOOH and 100 mM POBN, only a very weak ESR signal was recorded at pH 4.5 (Figure 5). The signal intensity was enhanced at a 10-fold higher concentration of the reactants, now clearly showing the spectrum of the well-known HO^\bullet radical adduct of POBN (**2**), with $a(\text{N}) = 15.01$ and $a(\text{H}) = 1.55$ G.⁶² According to spectral simulations, at least four other nitroxides (X_3 – X_6) were additionally produced in the course of peroxynitric acid decomposition (Figure 5). The ESR parameters (see Table S2) indicate (formal) adducts of (nitrogen-substituted) carbon-centered and probably nitrogen-centered radicals. Such species are reasonably explained by further oxidative conversion of POBN and/or POBN spin adducts by excess peroxynitric acid. The intermediacy of free HO^\bullet radicals during decomposition of O_2NOOH was further supported by experiments performed in the presence of DMSO. Initially after rapid mixing of peroxynitric acid with a solution of POBN and DMSO in phosphate buffer pH 4.5, a very intense three-line ESR spectrum of a nitroxide species (X_7) was monitored. The strong signals were accompanied by a number of weaker signals of other nitroxides (data not shown). The nitrogen hyperfine splitting [$a(\text{N}) = 12.87$ G] and the moderate lifetime (half-life ca. 10 min) rendered X_7 to be very similar to radical X_1 , observed with the spin trap DMPO under similar conditions (see above). Hence, it is very likely that with both spin trap compounds the same species has been trapped. At lower modulation, an additional splitting due to three equivalent hydrogens [$a(\text{H}) = 0.71$ G]

(60) NIEHS Spin-Trap DataBase; National Institute of Environmental Health Services, NIH: Research Triangle Park, NC; <http://mole.chem.bris.ac.uk/stdb/>.

(61) It cannot be excluded that DMPO–OH and DMPO–CH₃ indeed might have been formed in these experiments, because exploratory experiments in this laboratory showed that the ESR spectra of (independently generated) DMPO–OH as well as DMPO–alkyl radical adducts were rapidly destroyed on addition of peroxynitric acid, with concomitant buildup of the spectrum of **1**.

(62) Landolt-Börnstein, New Series, Group II, Magnetic Properties of Free Radicals, Vol. II/17d2; Fischer, H., Ed.; Springer-Verlag: Berlin, 1989; pp 81–88.

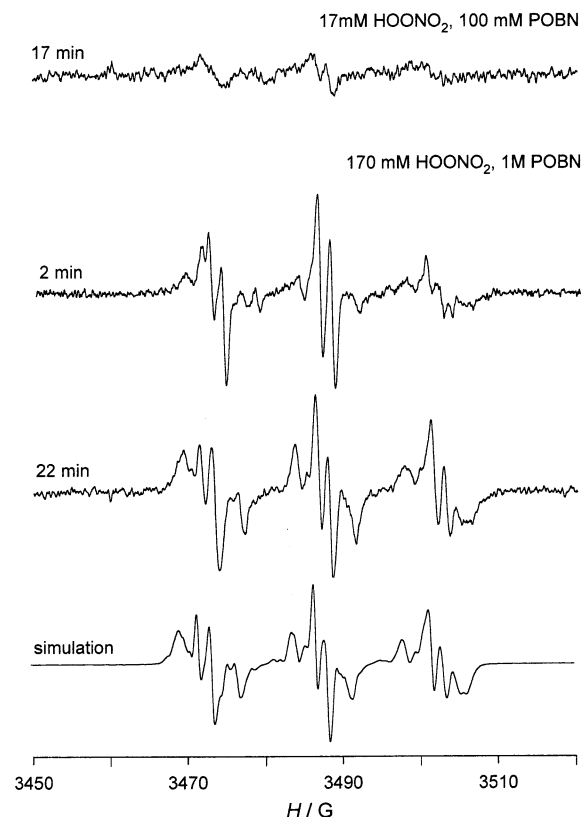


Figure 5. ESR spectra recorded at the times indicated after rapid mixing of 17 mM peroxyntic acid and 100 mM POBN and 170 mM peroxyntic acid and 1 M POBN, respectively, in phosphate buffer pH 4.5, $T = 20^\circ\text{C}$. ESR parameters evaluated by simulation are collected in Table S2.

was resolved. This splitting was absent in case of $[\text{D}_6]\text{DMSO}$ (see Figure S8), thus proving the trapping of a DMSO-derived radical. More importantly, the weaker, longer-lived spectral features were identified as due to the known methyl radical adduct of POBN, $\text{POBN}-\text{CH}_3$ (**3a**) [$a(\text{N}) = 15.82$, $a(\text{H}) = 2.62$ G].⁶² The release of methyl radicals from DMSO was unambiguously confirmed when $[\text{C}_2^{13}]\text{DMSO}$ was applied as hydroxyl radical scavenger. The ESR spectrum (Figure 6) now shows an additional doublet splitting as expected for $\text{POBN}-\text{C}^{13}\text{H}_3$ (**3b**) [$a(\text{C}^{13}) = 4.86$ G].⁶³ In accord, the ESR spectrum of $\text{POBN}-\text{CD}_3$ (**3c**), recorded in the presence of $[\text{D}_6]\text{DMSO}$ at pH 3.9 (Figure S8), was virtually identical to that of **3a** but showing smaller line widths. This indicates that unresolved splittings (≤ 0.4 G) due to the three methyl hydrogens contribute to the ESR line width of **3a**. In the experiments with $[\text{D}_6]\text{DMSO}$, a small signal of the carbonyl derivative of POBN (**4**) was also detected (Figure S8). Under otherwise identical conditions, the ESR signal intensities were much weaker at pH 1.9 (Figure S9). Initially after mixing, the superposition of the spectrum of (deuterated) X_7 and a 6-line spectrum with $a(\text{N}) = 14.02$ and $a(\text{H}) = 1.67$ G was observed. This spectrum decayed within 10 min. With regard to the hyperfine splittings⁶² and the rather short lifetime we tentatively assign the 6-line spectrum to the hydroperoxide adduct of POBN,

(63) This magnitude of the ^{13}C splitting agrees nicely with the splitting (4.24 G) predicted for **3a** by density functional theory (DFT) calculations on the B3LP/6-31G(d,p) level (H.-G. Korth, unpublished results).

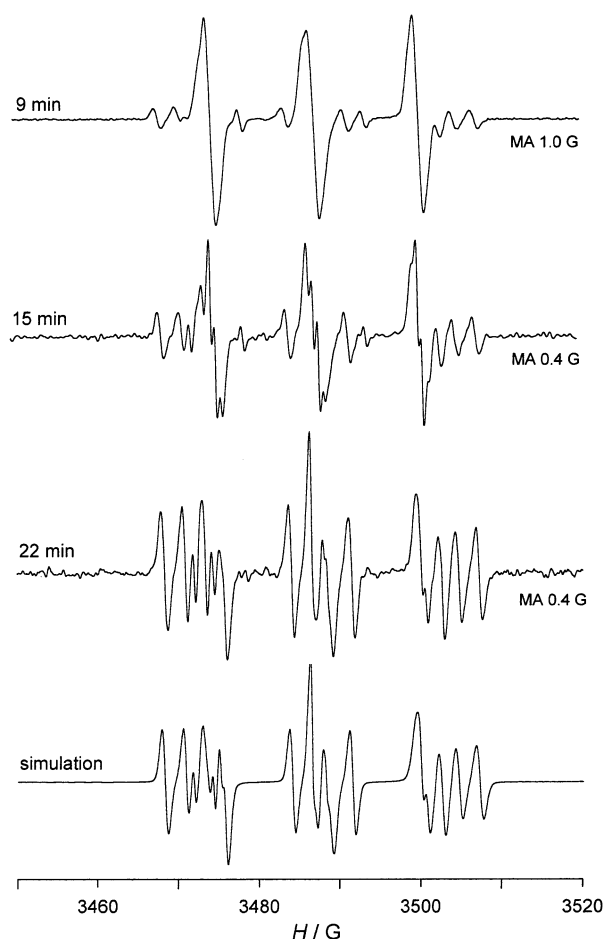


Figure 6. ESR spectra recorded at the times indicated after rapid mixing of 170 mM peroxyntic acid, 1 M POBN, and 2 M $[\text{C}_2^{13}]\text{DMSO}$ in phosphate buffer pH 4.5, $T = 20^\circ\text{C}$ (MA = modulation amplitude). ESR parameters evaluated by simulation are collected in Table S2.

$\text{POBN}-\text{OOH}$ (**5**). Weak signals of the $\text{POBN}-\text{CD}_3$ (**3c**) adduct grew in after a few minutes, accompanied by at least four other nitroxides (X_9 – X_{11}).⁶⁴ Thus, a low-level production of HO^\bullet and HOO^\bullet still seems to take place at this pH; however, the strongly decreased signal intensities are in line with the view that at low pH peroxyntic acid oxidizes DMSO preferably to dimethyl sulfone via a nonradical mechanism rather than to methane sulfinic/sulfonic acid via a radical route, as deduced from the above NMR product studies.

Conclusions

The ^{15}N CIDNP results presented here support the reported formation of peroxyntrous acid, the peroxyntrite– CO_2 adduct, and peroxyntic acid as rather short-lived intermediates during reaction of sodium nitrite with hydrogen peroxide in the pH range 3.1–5.25 and in the presence of carbon dioxide. The CIDNP experiments clearly demonstrate the

(64) The detection of the $\text{POBN}-\text{CD}_3$ radical adduct (**3c**) but not the $\text{POBN}-\text{OH}$ adduct (**2**) at the applied concentrations of POBN and $[\text{D}_6]\text{DMSO}$ agrees reasonably well with the relative magnitude of the rate constants of addition of HO^\bullet to POBN ($k = 4 \times 10^9 \text{ m}^{-1} \text{ s}^{-1}$)⁶⁵ and DMSO ($k = 7 \times 10^9 \text{ m}^{-1} \text{ s}^{-1}$),⁵⁷ respectively, i.e., a ca. four times preferred trapping of HO^\bullet by DMSO.

(65) Sridhar, R.; Beaumont, P. C.; Powers, E. L. *J. Radioanal. Nucl. Chem.* **1986**, *107*, 227.

Formation and Decay of Peroxynitric Acid

complexity and strong pH dependency of this reaction system. A decomposition path for peroxynitric acid via oxidation of its own anion to produce hydroxyl radicals is proposed. The intermediacy of HO• radicals is supported by NMR product studies and ESR spin-trapping experiments. Nitrogen dioxide, which probably represents the most important, though not only, nitrating agent of tyrosine residues in biological systems, is released by homolysis of all three intermediates in an acidic environment similar to that found in the stomach. However, at pH 7, where peroxynitric acid is largely deprotonated, both the release of HO• radicals and the oxidative power of peroxynitric acid are strongly reduced. The rather low oxidative power of O₂NOO⁻ is in full line with the recent view that radical recombination of O₂•⁻ and NO₂• represents at neutral pH values a deactivation mechanism for nitrogen dioxide in vivo.^{8,9}

Acknowledgment. We gratefully acknowledge the skillful technical assistance by Angela Wensing and Heinz Bandmann.

Supporting Information Available: Figures of the quantum-chemically computed structure of O₂NOOH⁻, 500 MHz ¹H NMR spectra after reaction of O₂NOOH with [¹³C₂]DMSO, ¹³C NMR spectra after reaction of O₂NOOH and ONOOH, respectively, with [¹³C₂]DMSO, and ESR spectra recorded during reaction of O₂NOOH with DMPO and POBN in the absence and presence of [¹³C₂]DMSO and [D₆]DMSO, respectively, and tables of (U)MP2/6-31+G(d,p)-computed Gibbs free energies and ESR data for DMPO and POBN spin trap adducts. This material is available free of charge via the Internet at <http://pubs.acs.org>.

IC020650Z